

# We are IntechOpen, the world's leading publisher of Open Access books Built by scientists, for scientists

6,900

Open access books available

186,000

International authors and editors

200M

Downloads

Our authors are among the

154

Countries delivered to

TOP 1%

most cited scientists

12.2%

Contributors from top 500 universities



WEB OF SCIENCE™

Selection of our books indexed in the Book Citation Index  
in Web of Science™ Core Collection (BKCI)

Interested in publishing with us?  
Contact [book.department@intechopen.com](mailto:book.department@intechopen.com)

Numbers displayed above are based on latest data collected.  
For more information visit [www.intechopen.com](http://www.intechopen.com)



# Synthesis and Characterization of CoO-ZnO-Based Nanocomposites for Gas-Sensing Applications

*Parthasarathy Panchatcharam*

## Abstract

CoO-ZnO composite nanofibers were synthesized through electrospinning technique. CoO-ZnO composite nanofibers were fabricated by doping zinc (zinc acetate dihydrate) and varied concentrations of cobalt (cobalt oxide) in the ratio of 1, 3, and 5 wt%, respectively. By modifying the solvent and the electrospinning parameters, different tests were carried out to optimize the morphological properties of the synthesized composite nanofibers. The morphological characterization was performed by scanning electron microscopy (SEM) with a field emission gun. The atomic composition of the nanofibers was analyzed by energy-dispersive X-ray (EDX) spectroscopy using a solid-state detector. Gas-sensing performances are done at different temperatures like at room temp, 50°C, and 100°C to find out the optimum operating temperature for detecting acetone gas. The sensitivity studies of CoO-ZnO composite nanofiber were carried out over different concentrations of acetone gas from 50 to 250 ppm. The sensitivity of this sensor developed is found to be increasing with increase in temperature and also increases if dopant concentration increases when compared with pure nanofibers. The sensitivity analysis proved a fact that uncalcinated CoO-ZnO composite nanofibers can be helpful in the detection of diabetics at the early stage with acetone concentration in the breaths.

**Keywords:** gas sensor, nanocomposites, metal oxide semiconductor, electrospinning, acetone sensing

## 1. Introduction

Semiconducting metal oxides have brought incredible attention as chemical sensors due to its characteristic resistivity and sensitivity changing features in an ambient environment [1, 2]. Being an N-type semiconductor, ZnO has been extensively used as a gas-sensing material owing to its wide band gap of 3.37 eV and high exciton binding energy of 60 meV at ambient temperature [3–9]. It has drawn tremendous attention in the last few decades due to its specific electrical, catalytic, and photochemical optoelectronic properties. It is the most widely studied semiconductor in gas-sensing applications because of its significant response to different reducing or oxidizing gases such as carbon monoxide, hydrogen, ammonia, ethanol, and acetone [10–12]. But some intrinsic disadvantages including high operating temperature, slow response and recovery time, and less sensitivity hinder the further advance in the development of ZnO-based gas sensors. So, boundless

efforts have been made in the last few years to overcome these limitations employing different methods, including noble metal doping, structure optimization, and heterostructure fabrication [13–15].

One such method to enhance gas-sensing properties is doping impurity elements [16]. Among the available methods for synthesizing nanostructures, electrospinning is a simple, adaptable, and low-cost technique for fabricating organic and inorganic nanofibers with significant lengths, uniform diameters, and various compositions [17]. During the electrospinning process, high voltage is applied to a polymer droplet being suspended at the tip of a syringe needle [18]. In this we present electrospun CoO-ZnO composite nanofibers with different concentrations like 1, 3, and 5 wt% of cobalt oxide. Calcination of cobalt oxide and zinc oxides leads to the formation of CoO-ZnO composite nanofibers having tunable diameters and significant porous structures. We studied the properties of the CoO-ZnO composite nanofibers fabricated, and specific dopants are used to improve the selectivity. The sensitivity of the nanofibers over acetone gas at lower concentrations has been examined, and the outcome of the fabricated nanofiber for sensing the acetone levels in breath of diabetic patients is sensed in low concentrations.

## 2. Related works

Alali et al. successfully synthesized ZnO/CoNiO<sub>2</sub> hollow nanofibers by an electrospinning method and postcalcination treatment. ZnO/CoNiO<sub>2</sub> hollow nanofibers gave an excellent response to ammonia solution, and further a great enhancement was achieved in ammonia sensing with these hollow fiber structures. ZnO/CoNiO<sub>2</sub> offered the best choice of ammonia-sensing materials by providing a response of 40 at 80°C [19]. Sun et al. synthesized pure and Er-doped ZnO nanofibers by electrospinning for high sensitivity detection of ethanol. They demonstrated that the diameter of the ZnO nanofibers decreases from 200 to 70 nm with the increase of Er content and the Er doping significantly increased the ethanol-sensing sensitivity of ZnO nanofibers at an optimum operating temperature of 240°C. This research also found that at the optimal Er content of 1.0 at%, the sensitivity of the nanofibers is 3.7 times larger than that of pure ones [20]. Wang et al. synthesized pure and Cu-doped ZnO fibers through electrospinning technology. The results of this research revealed that H<sub>2</sub>S gas-sensing properties of ZnO nanofibers were effectively improved by Cu doping: 6 at% Cu-doped ZnO nanofibers showed a maximum sensitivity to H<sub>2</sub>S gas, and the response to 10 ppm H<sub>2</sub>S is one order of magnitude higher than the one of pure ZnO nanofibers [21]. ZnO nanofibers were fabricated by an electrospinning method using a solution containing sol-gel precursors and solvent. It had been observed that the crystallinity of ZnO nanofibers improved with the increase in annealing temperature. The diameters of ZnO nanofibers after annealing above 600°C ranged from 35 to 100 nm. This work also confirmed the fact that the activation energy of ZnO nanofibers for electrical conduction was inversely proportional to the annealing temperature, and they also showed CO gas-sensing capacity at concentration as low as 1.9 ppm [22]. One-dimensional ZnO-SnO<sub>2</sub> hollow nanofibers were synthesized by Shouli bhai et al. by one-step electrospinning method and annealing treatment. The research depicted that the 20 atm% Zn composite not only exhibits the highest response that is 9 and 5.2 times higher than that of pristine ZnO and SnO<sub>2</sub>, respectively. It also exhibited rapid response, excellent selectivity, and stability at low operating temperature of 90°C, thereby promising to be a sensing material for the detection of NO<sub>2</sub> [23]. Pure and Ag-doped ZnO-SnO<sub>2</sub> hollow nanofibers had been synthesized through electrospinning method by Ma et al. The sensor based on the Ag-doped ZnO-SnO<sub>2</sub> hollow nanofibers exhibited excellent gas-sensing

performance at low operating temperature at 200°C and the fast response and recovery characteristics at low concentration of 1 ppm. This demonstrated that Ag-doped ZnO-SnO<sub>2</sub> could be used as a significant material for selective detection of low-concentration ethanol gas [24]. Moghaddam et al. synthesized polythiophene nanocomposite nanofibers containing ZnO nanoparticles through a self-assembly process in the presence of CTAB as the surfactant. Gas-sensing tests showed that the chemiresistor based on the as-prepared hybrid has high sensitivity, excellent repeatability, long-term stability, and short response time to ammonia gas at room temperature. ZnO/PT hybrid-sensing mechanism to ammonia gas was presumed to be the effect of p-n heterojunction between ZnO nanoparticles and PT [25]. Nano-crystalline ZnO nanofiber mats were synthesized through combined sol-gel electrospinning techniques followed by calcination in which poly(styrene-co-acrylonitrile) and zinc acetate were used as the binder and precursor, respectively. The average diameter of the ZnO nanofibers decreased from 400 to 60 nm, while their grain size and crystallinity were enhanced by increasing the calcination temperature. Due to their high surface area and superhydrophilicity, these ZnO nanofiber mats were highly sensitive in sensing gaseous ammonia, and the sensitivity of these mats increased as a function of their calcination temperatures [26].

### 3. Experimental

#### 3.1 Preparation of Co-doped ZnO composite nanofibers

The fabrication of CoO-ZnO composite nanofibers was achieved by electrospinning followed by calcination. In this 0.595 g of zinc acetate dihydrate and varied concentrations of cobalt oxide in the ratio of 1, 3, and 5 wt% were added to 10 ml of dimethylformamide solvent. All the reagents were purchased from Sigma-Aldrich Corporation. The solution was magnetically stirred for 5–6 hours at room temperature; subsequently 1 g of polyvinylpyrrolidone (PVP) and 8 ml of were added to the mixture and kept for further stirring of about 2–3 hours at room temperature. The resulting solutions were electrospun using commercial electrospinning apparatus (EC-DIG Electrospinning, IME Technologies). The composites were ejected from the needle of a syringe applying an electrical field, as high voltage of about 18 kV and at the needle with collector distance of 20 cm. Composite nanofibers were collected in the stationary mode on the surface of silicon substrates clamped on top of a conductive circular collector.

By modifying the solvent and the electrospinning parameters, different tests were carried out to optimize the morphological properties of the synthesized composite nanofibers. While decomposition, we employed a negative and positive voltage between the needle and the substrates was 14–20 cm, and the flow of the solutions were set to 5 µl/min. The deposition times were kept constant at 3 min. The morphological characterization was performed by scanning electron microscopy (SEM) with a field emission gun. The atomic composition of the nanofibers was analyzed by energy-dispersive X-ray (EDX) spectroscopy using a solid-state detector. Gas-sensing performances are done at different temperatures like at room temp, 50°C, and 100°C to find out the optimum operating temperature for detecting acetone gas. The sensitivity studies of CoO-ZnO composite nanofiber were carried out over different concentrations of acetone gas from 50 to 250 ppm.

#### 3.2 Gas-sensing mechanism

When Zn and O combine, Zn loses two valence electrons to O; thus, due to loss of an outer shell, the Zn atom shrinks in size, while O atom increases in size due



to addition of an outer shell. The wide difference in size between zinc and oxygen atom will allow large space while providing foreign atoms to incorporate. Cobalt oxide-zinc oxide composite in the presence of ambient oxygen undergoes chemical absorptive changes by capturing electrons in conduction band which is known as recombination where oxygen molecule is adsorbed on its surface. This will decrease the barrier height for electrons to transport there by reducing the resistance value.

Activation energy is required for adsorption and desorption of oxygen and detection of gas. This in turn will control the recovery time and response as well. Temperature plays a major role in controlling this mechanism. The basic sensing mechanism in this thin-film sensors includes that at temperature which is less than or equal to 100°C where the adsorption mechanism takes place, that is, acetone gas passes over the sensing film oxygen molecules such as  $O_2^-$  will form and upon increase in temperature it will get modified to  $2O^-$  and then  $O_2^-$ . Then in the presence of acetone gas, carbon dioxide gas is released and water and electrons are gained. In oxidizing mechanism,  $O_2$  atoms will be gained and in reduction mechanism atoms will be lost.

Mostly semiconducting gas-detecting sensors, resistance will change according to the adsorption and desorption of gas molecules on the surface of the thin film [26–29]. The ZnO nanofibers in the presence of air ambience will absorb the oxygen on the surface of the thin film. Later by collecting electrons from the conductance band, the oxygen adsorbed is changed into various chemical states. Thus, the nanofibers will show more resistance with the increment of the barrier height of  $e^-$  to move. Since the target gas acetone is a reducing gas, the oxygen which is adsorbed on the surface will undergo oxidation with acetone. In this reaction resistance of sensor will reduce when  $e^-$  enters the nanofibers as depicted in **Figure 1**.

The structure of the fibers plays a very vital role in getting sensitivity. Since the ZnO thin films will have high surface to volume ratio will have high sensing performance. Many earlier papers discussed about the ZnO thin film in sensing different gases. In this case the electrospinning technique used to synthesize nanofibers with various parameters will improve the sensor sensitivity for 5 wt% CoO-ZnO-calcinated nanofibers. Cobalt oxide is preferred in here to increase the catalytic conversion when compared with other dopants like Ni, Al, etc.

### 3.3 Fabrication of gas sensor

The calcinated sample in the form of thin film is fabricated to form a handheld sensor for sensing the acetone gas. Here, the thin film is placed over a glass substrate and upon the masks of desire pattern is placed as shown in **Figure 2**. The physical vapor deposition technique, a thermal evaporation process, is followed for the fabrication of the thin films. The masks were prepared by using  $CO_2$  laser technique of comb pattern using acrylic sheet. Later the mask is placed on the thin film and these sensing materials are placed on the sample holder. Physical vapor deposition technique is followed for vaporization of the thin films where higher pressure is applied under higher temperature in a vacuum chamber. Indium electrodes were fixed by microsoldering technique, and copper leads were separated from the electrodes. The sensor is heated by placing upon a hot ceramic plate at 200°C.

Gas-sensing chamber has an inlet and an outlet chamber where the target gas is sent through an inlet nozzle. The sample is placed inside the chamber, and the two probes of electrometer were connected to the copper wires to measure the change in the resistance variation. One of the input parameters is the input voltage of about 3v; accordingly corresponding change in resistance and time variation is noted by injecting acetone of liquid form upon heating becomes gaseous state.

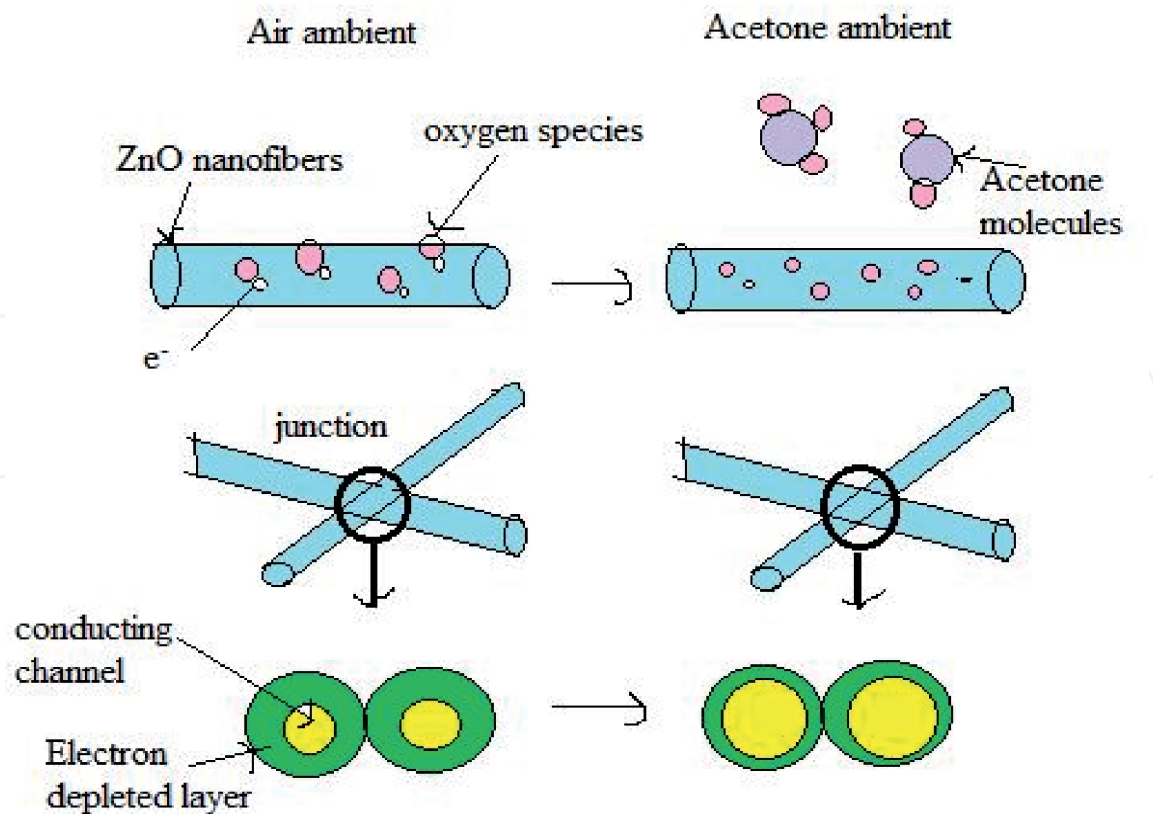


**Figure 1.**  
*Schematic sensing process of ZnO nanofibers.*

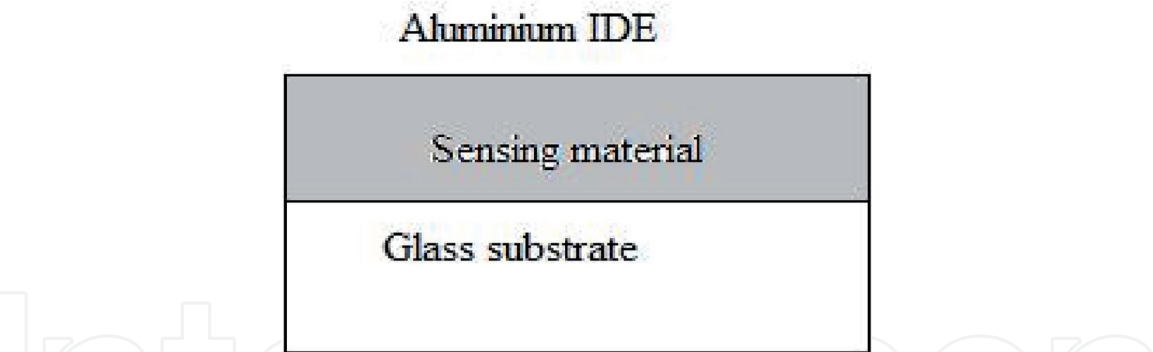


**Figure 2.**  
*Schematic of gas sensor.*

The sensor resistances were calculated automatically by analysis system. The acetone liquid was injected in different concentrations of about 10, 50, 100, 150, 200, and 250 ppm. According to the volume of the chamber, this conversion is done, i.e., ml to ppm. This process is repeated at room temperature, 50°C, and 100°C by using ceramic heater to obtain the optimum temperature. The process is repeated until the gas evaporates properly from the gas chamber. The sensitivity is calculated by using the following formula:

$$S (\%) = (R_a - R_g / R_a) \times 100 \tag{1}$$

R<sub>a</sub>—Resistance in air ambience.  
R<sub>g</sub>—Resistance in the presence of target gas.



4. Results and discussion

The morphological, structural, and thermal analyses are discussed in this section.

4.1 Morphological analysis of the as-prepared Co-doped ZnO nanofibers

Typical scanning electron microscopy (SEM) images of the synthesized nanofibers of pure ZnO nanofiber and cobalt-doped composite nanofibers of purity in the ratio of 1, 3, and 5 wt%, respectively, were shown in **Figure 3**. The nanofibers have a random orientation, as expected, due to the instability of the electrospinning jet. The EDX analysis (**Figure 4**) shows the presence of carbon, nitrogen, zinc, cobalt, and oxygen coming from PVP, zinc acetate, and cobalt oxide, respectively. The porosity of the electrospun mats is confirmed by detection of silicon signal

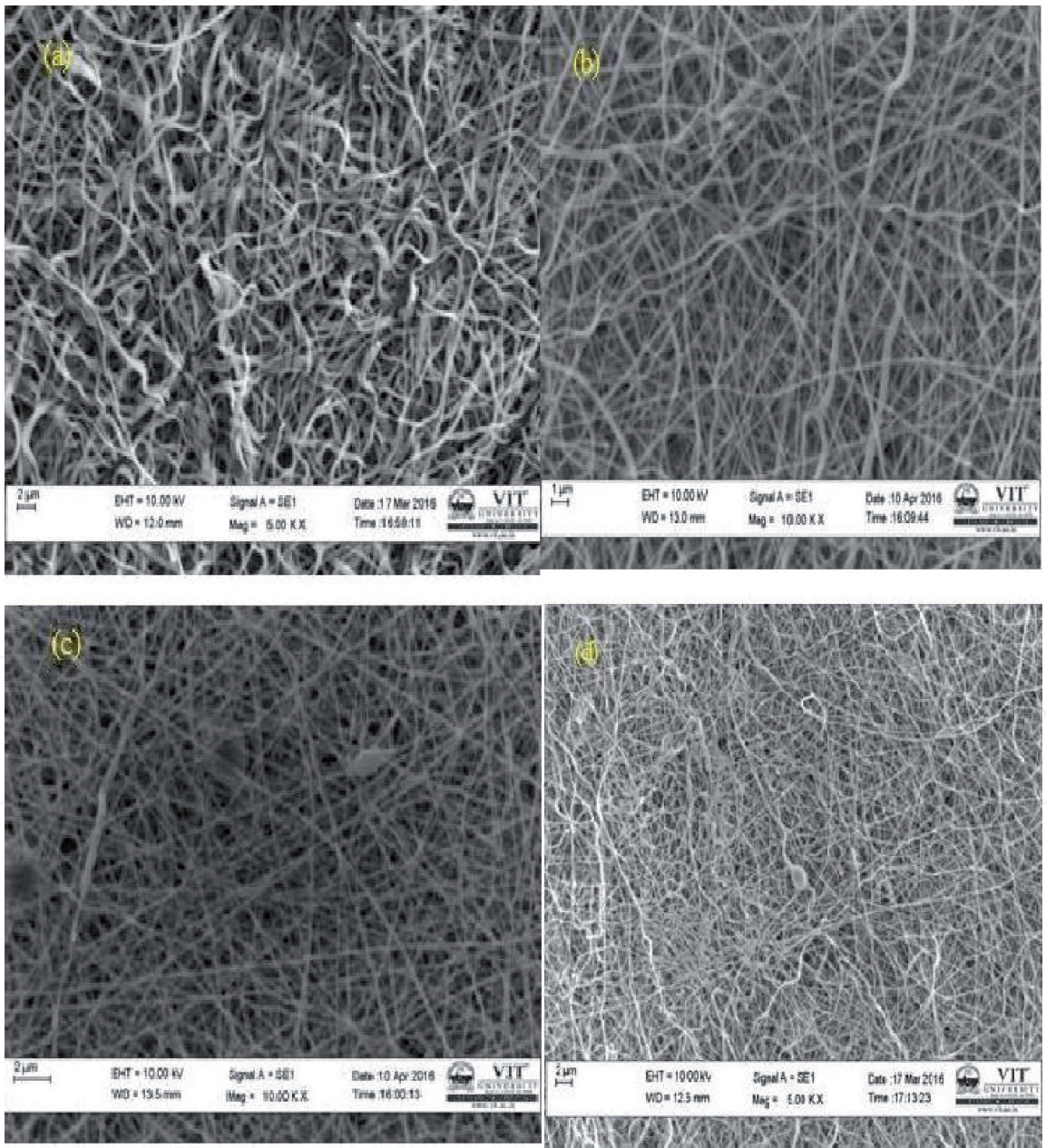


**Figure 3.** (a) Pure ZnO-calcinated fiber, (b) 1 wt% CoO-ZnO-calcinated nanofibers, (c) 3 wt% CoO-ZnO-uncalcinated nanofibers, and (d) 5 wt% calcinated CoO-ZnO composite nanofiber.

coming from the substrate. The diameter of the nanofibers fabricated appears to be uniform, and it is also evident that it becomes thinner upon the increase of dopant concentration, i.e., 1 wt% CoO, 2 wt% CoO, and 5 wt% CoO, respectively. This is the result of addition of charges increased during the electrospinning process. Furthermore, a typical EDX spectrum of the Co-doped ZnO nanofibers was illustrated in **Figure 4(d)**, which shows only the peaks associated with Zn, Co, and O atoms (Cu is from copper mesh grids) were detected. Therefore, the nanofibers were indeed Co-doped ZnO materials.

#### 4.2 Thermogravimetric analysis of the as-prepared nanofibers

Thermogravimetric (TG) analysis was performed on a NET-ZSCH STA 449 thermo-analyzer in an air atmosphere. The precursor fibers of PVP/zinc acetate/cobalt acetate composite produced after electrospinning must be annealed because of its high contents of organic polymer and ethanol solvents in these nanofibers. The thermal behavior of the precursor fibers of this composite is shown in **Figure 5**; it illustrates that most of the organics belonged to PVP and the CH<sub>3</sub>COO group and other volatiles (H<sub>2</sub>O, CO<sub>2</sub>, etc.) are detached at temperature < 600°C. Beyond 600°C, there is no change in weight loss, indicating the formation of pure inorganic oxide. The XRD curve depicted in **Figure 6** shows all the peak positions of Co-doped ZnO nanofibers which suggested that Co is successfully incorporated into the crystal lattice of ZnO which is reasonable given that the ionic radii of tetrahedrally coordinated Co<sup>2+</sup> and Zn<sup>2+</sup> are similar.

#### 4.3 Optical properties of the as-prepared nanofibers

Optical properties of ZnO nanofibers and Co-doped ZnO nanofibers have been examined through Raman spectrometers and photoluminescence (PL). **Figure 7** shows their typical PL spectra under an excitation wavelength of 325 nm; only a broad and strong ultraviolet (UV) luminescence with a maximum at 375 nm is observed. This ascribed to the near band edge emission of the wide band gap zinc oxide. Compared to the spectrum of ZnO nanofibers formed under the same experimental condition, the emission peak of Co-doped nanofibers is shifted about 10 nm toward longer wavelength significantly. ZnO powders are heavily doped by donors like In, and it was interpreted as mainly due to the sp-d exchange interactions between the band electrons and the localized d electrons of the Co<sup>2+</sup> ions substituting Zn ions. The s-d and p-d exchange interactions lead to a negative and a positive correction to the conduction band and the valence band edges, resulting in a band gap narrowing.

To confirm that the Co ions as the dopant were successfully incorporated into the crystal lattice of ZnO, Raman scattering spectra of ZnO nanofibers and Co-doped ZnO nanofibers were measured. As observed in **Figure 8(a and b)**, the Raman spectrum of the ZnO nanofibers exhibits a strong peak at 437 cm<sup>-1</sup>, which has been assigned to the vibration mode E<sub>2</sub> (H) characteristic of the ZnO with hexagonal structure. The peaks at 330 and 379 cm<sup>-1</sup> are assigned to the vibration mode 2E<sub>2</sub> and the A<sub>1</sub> (TO) mode, respectively. In comparison to the Raman spectrum of ZnO nanofibers, most modes in Co-doped ZnO nanofibers figure, expecting the A<sub>1</sub> (TO) mode is disappeared. The E<sub>2</sub> (H) mode and the vibration mode 2E<sub>2</sub> broaden asymmetrically and shift toward lower frequencies when the Co is doped. This is due to the broken symmetry induced by the incorporation of Co dopants into the ZnO structure and could be explained by the



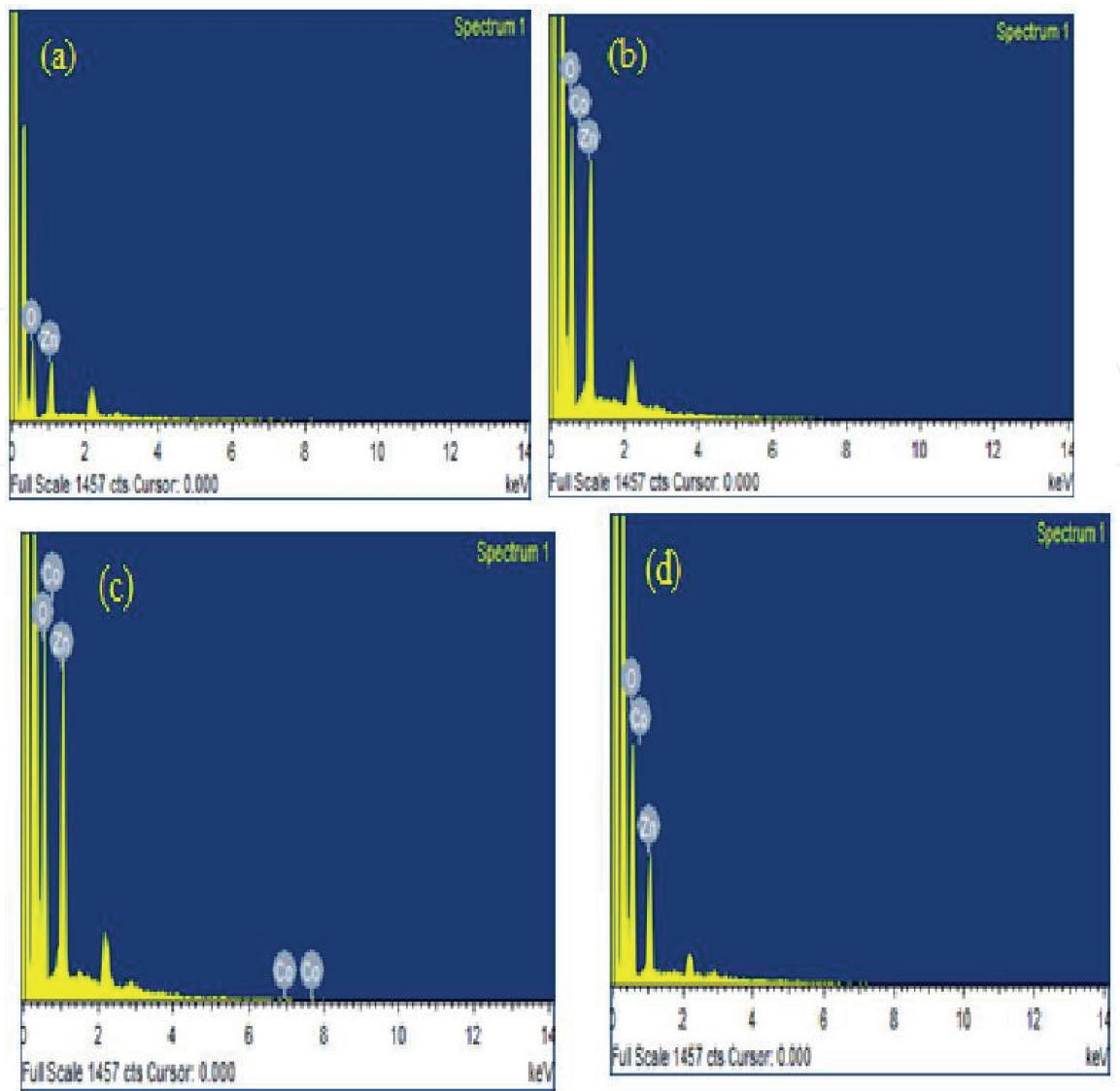


**Figure 4.** EDX analysis: (a) ZnO-calcinated fiber, (b) 1 wt% CoO-ZnO-calcinated nanofibers, (c) 3 wt% CoO-ZnO-calcinated nanofibers, and (d) 3 wt% CoO-ZnO-uncalcinated nanofibers.

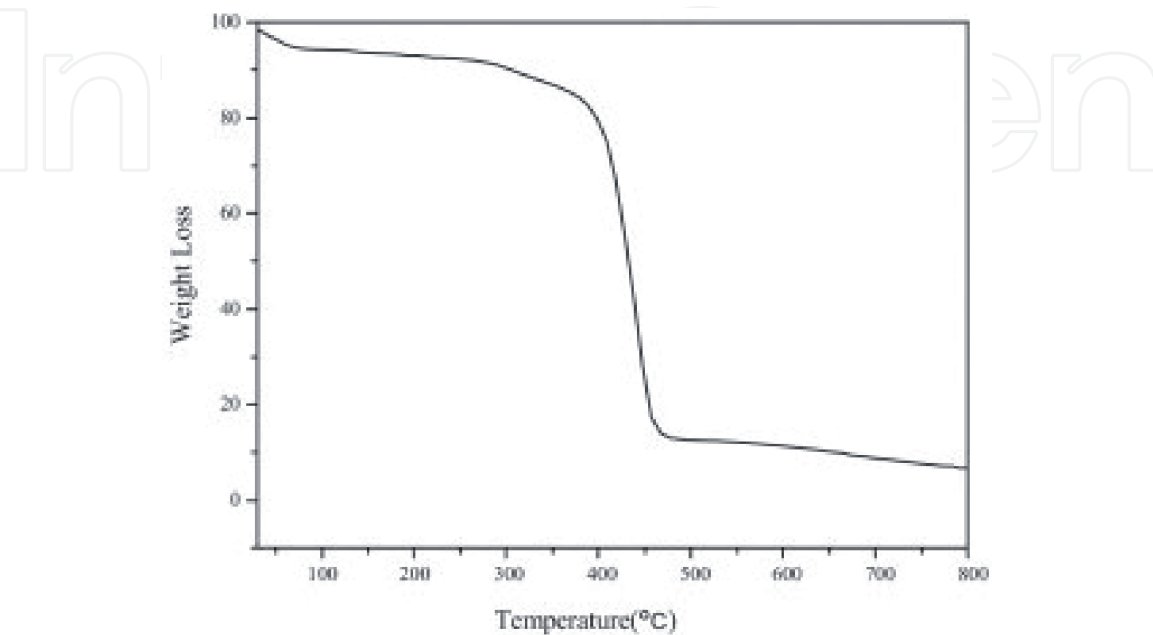


**Figure 5.** TG curves of precursor fibers of PVP/zinc acetate/cobalt acetate composites.

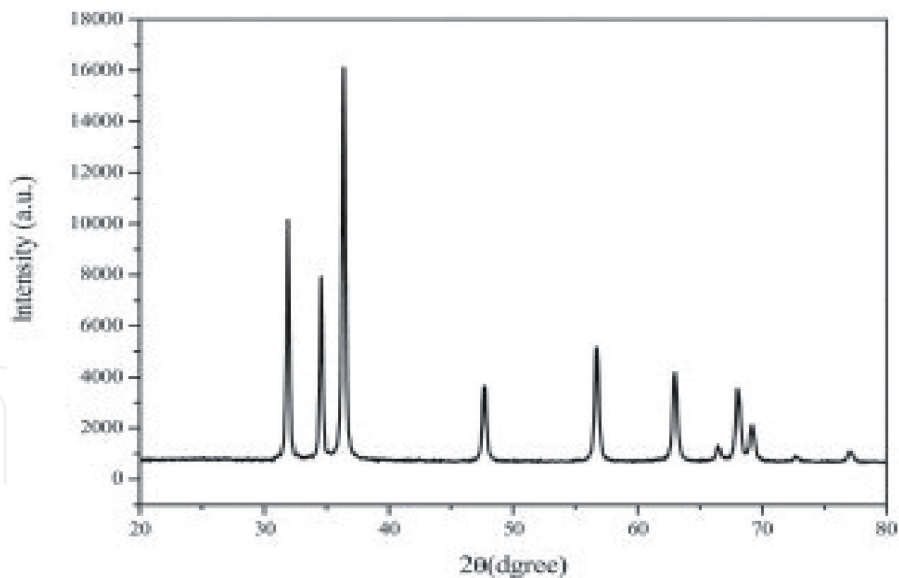


**Figure 6.**  
*XRD of Co-doped ZnO nanofibers after calcination at 600°C.*

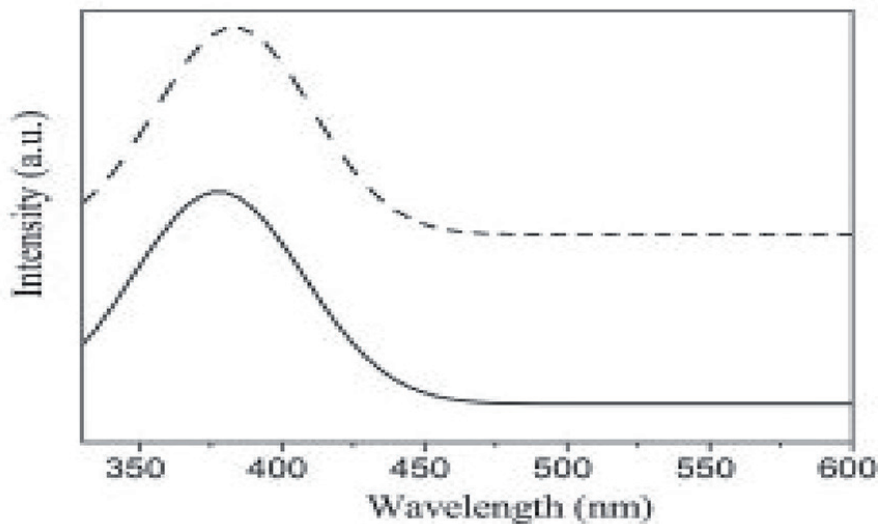


**Figure 7.**  
*PL structures of ZnO nanofibers (solid line) and Co-doped ZnO (dotted lines) after calcination at 600°C.*

spatial-correlation model [30, 31]. Apart from these features, the Co-doped ZnO nanofibers exhibit an unusual peak at  $540\text{ cm}^{-1}$ , which has been assigned to the quasi-LO phonon mode (AM1) due to the abundant shallow donor defects, such as oxygen vacancies or zinc interstitials bounded on the tetrahedral Co sites [32]. These results together confirm that Co was successfully doped into the crystal lattice of ZnO nanofibers.

#### 4.4 Gas-sensing performance analysis

Gas-sensing performances were performed at different temperatures of ambient, 50°C, and 100°C to find out the optimum operating temperature for the detection of acetone gas. The sensitivity plots were measured for concentration of acetone gas against purity of the CoO-ZnO nanocomposite fibers fabricated. The sensitivity of the dopants was found to be increasing with increase in temperature and increases with the increase in dopant concentration when compared with the pure nanofibers.

When the operating temperature is low, the activation energy used will be reduced simultaneously, and in turn the response will be decreased. At the same time, if the operating temperature used is very high due to the increased activation energy, the adsorbed gas molecules will escape before the reaction occurs; thus, the response will decrease too. In this chapter, 5 wt% calcinated CoO-ZnO nanofibers at 100°C have high sensitivity when compared with other compositions like pure, 1, and 3 wt%. Hence this sample can be improvised to make use in many applications like diabetic's detection where the ppm range should be between 1 and 3 ppm. The base resistance, i.e., in the presence of air ambience, will increase and in the presence of acetone gas will increase. Since the acetone gas will evaporate if exposed to air temperature, the gas injected should be properly according to time to time. The ppm is calculated according to the gas chamber volume. According to the volume of the gas chamber used in this chapter, the ppm is taken as 5 ml as 50 ppm. Acetone is calculated in terms of parts per million. The main feature of this chapter is to improvise the selectivity of acetone sensing with CoO-ZnO nanofibers.

**Figure 9** shows the sensor sensitivity for pure ZnO nanofibers. In this plot the sensitivity will increase linearly from 50 to 250 ppm with increase in the acetone

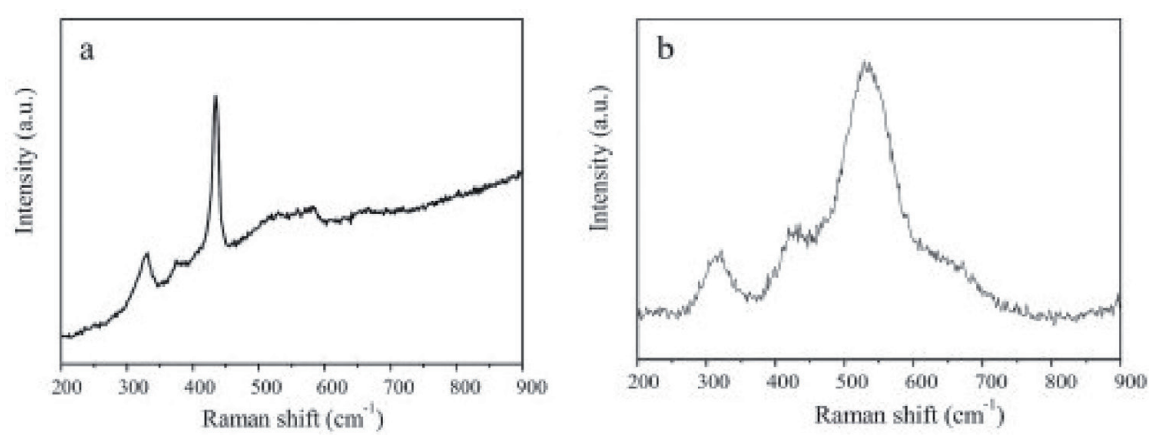


**Figure 8.**  
Raman spectra of (a) ZnO nanofibers and (b) Co-doped ZnO nanofibers after calcination at 600°C.

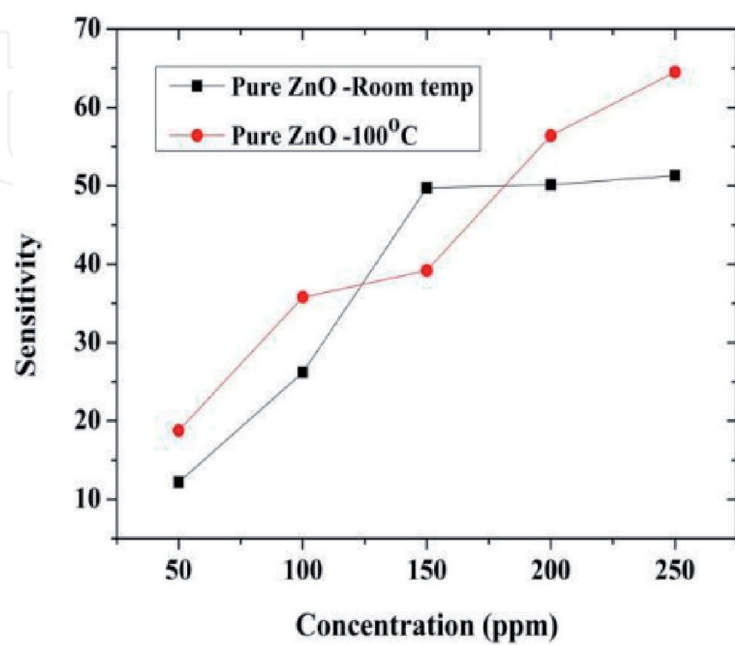


**Figure 9.**  
Sensitivity plot for pure ZnO nanofibers.



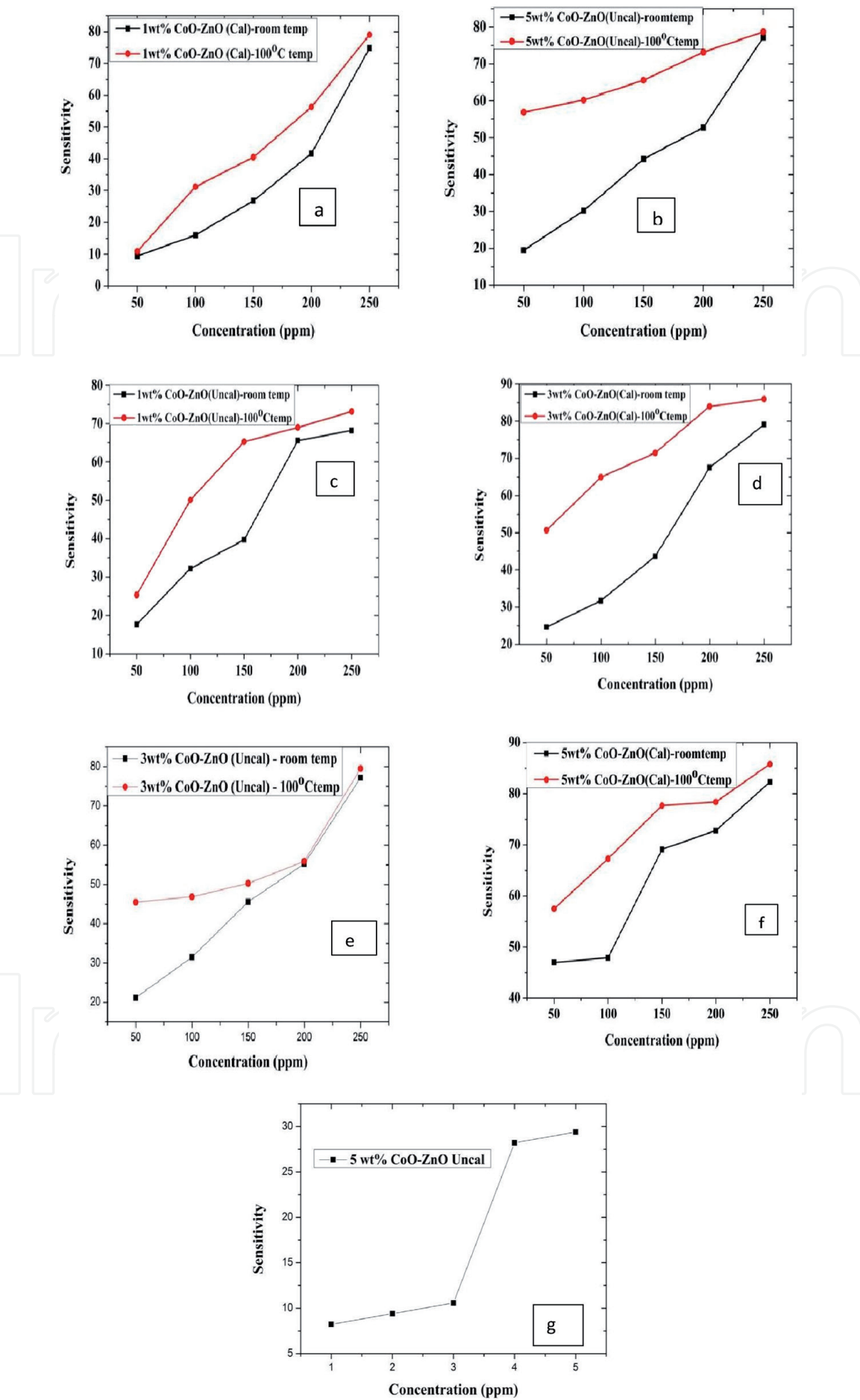


**Figure 10.**  
Sensitivity plots: (a) 1 wt% CoO-ZnO uncal, (b) 1 wt% CoO-ZnO cal, (c) 3 wt% CoO-ZnO uncalcinated, (d) 3 wt% CoO-ZnO cal, (e) 5 wt% CoO-ZnO uncalcinated, (f) 5 wt% CoO-ZnO calcinated, and (g) 5 wt% CoO-ZnO uncalcinated.

concentration. Such linear sensitivity will be helpful in sensing gases like acetone. When compared with that of the room temperature, pure ZnO nanofibers will show high sensitivity at 100°C. The plot is between concentrations in ppm vs. sensitivity.

From **Figure 10(a–g)**, the plots for 1, 3, and 5 wt% for both calcinated and uncalcinated, the sensitivity will linearly increase with increase in concentration and also increase if the dopant concentration increases along with the operating temperature increases, i.e., at the 100°C temperature.

The above plot gives details about sensitivity plot for 5 wt% CoO-ZnO-uncalcinated nanofibers at concentration from 1 to 5 ppm where the linearity increment will be there from 3 to 5 ppm which is helpful in many applications in medical field like in diabetic's detection.

## 5. Conclusion


SEM analysis is used to determine the composition, structure, and surface morphologies of fibers. The amount of acetone in ppm range is detected. The sensitivity, change in resistance, and variation of calcinated and uncalcinated fibers were analyzed. The analyses which were taken from these results, that is, change in calcinated nanofibers, show more response to acetone when compared with uncalcinated nanofibers. The reason behind this kind of statement is PVP decomposed on calcination and hence it shows more resistivity, whereas in the case of uncalcinated fibers, PVP will not allow the zinc oxide to respond. From the sensitivity plots, we note that sensitivity increases when the doping concentration increases but also increases in the case of calcinated fibers. This chapter will discuss the pure, 1, 3, and 5 wt% CoO-ZnO nanofibers for acetone detection. The results give information that 5 wt% CoO-ZnO nanofibers will improve the acetone-sensing performances efficiently even if the atmosphere is complicated. These results will be helpful in many acetone gas-sensing applications widely.

## Author details

Parthasarathy Panchatcharam  
Research Scholar, School of Electrical Engineering, VIT University, Vellore,  
Tamil Nadu, India

\*Address all correspondence to: arjunsarathii@gmail.com

## IntechOpen

© 2020 The Author(s). Licensee IntechOpen. Distributed under the terms of the Creative Commons Attribution - NonCommercial 4.0 License (<https://creativecommons.org/licenses/by-nc/4.0/>), which permits use, distribution and reproduction for non-commercial purposes, provided the original is properly cited. 

## References

- [1] Lee JH. Gas sensors using hierarchical and hollow oxide nanostructures: Overview. *Sensors and Actuators B: Chemical*. 2009;**140**:319-336
- [2] Choi SJ, Choi CY, Kim SJ, Cho HJ, Hakim M, Jeon S, et al. Highly efficient electronic sensitization of non-oxidized graphene flakes on controlled pore-loaded WO nanofibers for selective detection of H<sub>2</sub>S molecules. *Scientific Reports*. 2015;**5**:8067. DOI: 10.1038/srep08067
- [3] Liang YC, Liao WK, Deng XS. Synthesis and substantially enhanced gas sensing sensitivity of homogeneously nanoscale Pd- and Au-particle decorated ZnO nanostructures. *Journal of Alloys and Compounds*. 2014;**599**:87-92
- [4] Gardon M, Guilemany JM. A review on fabrication, sensing mechanisms and performance of metal oxide gas sensors. *Journal of Materials Science*. 2013;**24**:1410-1421. DOI: 10.1007/s10854-012-0974-4
- [5] Hu J, Gao FQ, Sang SB, Li PW, Deng X, Zhang WD, et al. Optimization of Pd content in ZnO microstructures for high-performance gas detection. *Journal of Materials Science*. 2015;**50**:1935-1942. DOI: 10.1007/s10853-014-8758-2
- [6] Wang WC, Tian YT, Wang XC, He H, Xu YR, He C, et al. Ethanol sensing properties of porous ZnO spheres via hydrothermal route. *Journal of Materials Science*. 2013;**48**:3232-3238. DOI: 10.1007/s10853-012-7103-x
- [7] Khoang ND, Hong HS, Trung DD, Duy NV, Hoa ND, Thinh DD, et al. On-chip growth of wafer-scale planar-type ZnO nanorod sensors for effective detection of CO gas. *Sensors and Actuators B: Chemical*. 2013;**181**:529-536
- [8] Zhang WH, Zhang WD, Zhou JF. Solvent thermal synthesis and gas-sensing properties of Fe-doped ZnO. *Journal of Materials Science*. 2010;**45**:209-215. DOI: 10.1007/s10853-009-3920-y
- [9] Luo J, Ma SY, Li FM, Li XB, Li WQ, Cheng L, et al. The mesoscopic structure of flower-like ZnO nanorods for acetone detection. *Materials Letters*. 2014;**121**:137-140
- [10] Zhang Y, Xu J, Xiang Q, Li H, Pan Q, Xu P. Brush-like hierarchical ZnO nanostructures: synthesis, photoluminescence and gas sensor properties. *The Journal of Physical Chemistry C*. 2009;**113**(9):3430-3435
- [11] Bal AK, Singh A, Bedi RK. Characterization and ammonia sensing properties of pure and modified ZnO films. *Applied physics A*. 2011;**103**(2):497-503
- [12] Subannajui K, Wongchoosuk C, Ramgir N, Wang C, Yang Y, Hartel A, et al. Photoluminescent and gas-sensing properties of ZnO nanowires prepared by an ionic liquid assisted vapor transfer approach. *Journal of Applied Physics*. 2012;**112**(3):034311
- [13] Song N, Fan HQ, Tian HL. PVP assisted in situ synthesis of functionalized graphene/ZnO (FGZnO) nanohybrids with enhanced gas-sensing property. *Journal of Materials Science*. 2015;**50**:2229-2238. DOI: 10.1007/s10853-014-8785-z
- [14] Tarwal NL, Rajgure AV, Patil JY, Khandekar MS, Suryavanshi SS, Patil PS, et al. A selective ethanol gas sensor based on spray-derived Ag-ZnO thin films. *Journal of Materials Science*. 2013;**48**:7274-7282. DOI: 10.1007/s10853-013-7547-7



- [15] Zhang ZY, Li XH, Wang CH, Wei LM, Liu YC, Shao CL. ZnO hollow nanofibers: Fabrication from facile single capillary electrospinning and applications in gas sensors. *The Journal of Physical Chemistry C*. 2009;**113**:19397-19403
- [16] Yamazoe N. New approaches for improving semiconductor gas sensors. *Sensors and Actuators B: Chemical*. 1991;**5**(1-4):7-19
- [17] Chen QL, Lai X, Yan ML, Tang GR, Luo JY, Chen J, et al. Preparation of tungsten oxide nanoplate thin film and its gas sensing properties. In *Advanced Materials Research*. Vol. 774. Trans Tech Publications; 2013. pp. 687-690
- [18] Teo WE, Ramakrishna S. A review on electrospinning design and nanofibre assemblies. *Nanotechnology*. 2006;**17**(14):R89
- [19] Alali KT, Liu T, Liu J, Liu Q, Fertassi MA, Li Z, et al. Preparation and characterization of ZnO/CoNiO<sub>2</sub> hollow nanofibers by electrospinning method with enhanced gas sensing properties. *Journal of Alloys and Compounds*. 2017;**702**:20-30
- [20] Sun Y, Zhao Z, Li P, Li G, Chen Y, Zhang W, et al. Er-doped ZnO nanofibers for high sensibility detection of ethanol. *Applied Surface Science*. 2015;**356**:73-80
- [21] Zhao M, Wang X, Ning L, Jia J, Li X, Cao L. Electrospun Cu-doped ZnO nanofibers for H<sub>2</sub>S sensing. *Sensors and Actuators B: Chemical*. 2011;**156**(2):588-592
- [22] Park JA, Moon J, Lee SJ, Lim SC, Zyung T. Fabrication and characterization of ZnO nanofibers by electrospinning. *Current Applied Physics*. 2009;**9**(3):S210-S212
- [23] Zhao Y, Li X, Dong L, Yan B, Shan H, Li D, et al. Electrospun SnO<sub>2</sub>-ZnO nanofibers with improved electrochemical performance as anode materials for lithium-ion batteries. *International Journal of Hydrogen Energy*. 2015;**40**(41):14338-14344
- [24] Ma L, Ma SY, Kang H, Shen XF, Wang TT, Jiang XH, et al. Preparation of Ag-doped ZnO-SnO<sub>2</sub> hollow nanofibers with an enhanced ethanol sensing performance by electrospinning. *Materials Letters*. 2017;**209**:188-192
- [25] Moghaddam HM, Malkeshi H. Self-assembly synthesis and ammonia gas-sensing properties of ZnO/Polythiophene nanofibers. *Journal of Materials Science: Materials in Electronics*. 2016;**27**(8):8807-8815
- [26] Senthil T, Anandhan S. Structure-property relationship of sol-gel electrospun ZnO nanofibers developed for ammonia gas sensing. *Journal of Colloid and Interface Science*. 2014;**432**:285-296
- [27] Egashira M, Kanehara N, Shimizu Y, Iwanaga H. Gas-sensing characteristics of Li<sup>+</sup>-doped and undoped ZnO whiskers. *Sensors and Actuators B: Chemical*. 1989;**18**:349-360
- [28] Franke ME, Koplin TJ, Simon U. Metal and metal oxide nanoparticles in chemiresistors: Does the nanoscale matter? *Small*. 2006;**2**:36-50
- [29] Barsan N, Koziej D, Weimar U. Metal oxide-based gas sensor research: How to? *Sensors and Actuators B: Chemical*. 2007;**121**:18-35
- [30] Parayanthal P, Pollak FH. Raman scattering in alloy semiconductors: "Spatial correlation" model. *Physical Review Letters*. 1984;**52**(20):1822-1825
- [31] Phan TL, Yu SC, Vincent R, Bui HM, Thanh TD, Lam VD, et al. Influence of Mn doping on structural, optical, and magnetic properties of Zn<sub>1-x</sub>Mn<sub>x</sub>O

nanorods. Journal of Applied Physics.  
2010;**108**(4):044910-044916

[32] Wang X, Xu J, Yu X, Xue K, Yu J,  
Zhao X. Structural evidence of  
secondary phase segregation from the  
Raman vibrational modes in  $\text{Zn}_{1-x}\text{Co}_x\text{O}$  ( $0 < x < 0.6$ ). Applied Physics  
Letters. 2007;**91**(3):031908-031910